Available online at www.sciencedirect.com
SCIENCE DIRECT
Catalysis Today 110 (2005) 351–356
CATALYSIS TODAY
www.elsevier.com/locate/cattod

Selective oxidation of cyclohexane in supercritical carbon dioxide over CoAPO-5 molecular sieves

Ruizhen Zhang, Zhangfeng Qin, Mei Dong, Guofu Wang, Jianguo Wang *

State Key Laboratory of Coal Conversion, Institute of Coal Chemistry, Chinese Academy of Sciences, P.O. Box 165, Taiyuan, Shanxi 030001, PR China

Available online 24 October 2005

Abstract

A series of cobalt-incorporated aluminophosphates (CoAPO-5) with different Co contents were hydrothermally synthesized. The tetrahedral Co^{2+} in the lattice framework was evidenced by various spectroscopic characterizations, which could be partially oxidized to Co^{3+} to form redox centers upon calcination. Over CoAPO-5, the selective oxidation of cyclohexane was carried out with CO_2 as an additional solvent under supercritical conditions, where the different phase regions were categorized by the critical properties of the nominal reacting mixture (cyclohexane + nitrogen + carbon dioxide + cyclohexanol + cyclohexanone + water) that varies with the reaction extent. The results indicated that CoAPO-5 is an effective catalyst for the selective oxidation of cyclohexane to cyclohexanol and cyclohexanone; in the compressed CO_2, the total selectivity of objective products increased and the by-products were suppressed considerably. The conversion of cyclohexane decreased, while the selectivity to cyclohexanol and cyclohexanone increased with the increase of the apparent density.

Keywords: Selective oxidation; CoAPO-5 molecular sieve; Cyclohexane; Carbon dioxide; Supercritical; Cyclohexanol; Cyclohexanone

1. Introduction

The selective oxidation of cyclohexane into cyclohexanol (-ol) and cyclohexanone (-one) is of considerable importance in the chemical industry for producing Nylon-6 polymers. Most of the current processes still use ''sacrificial'' oxidants like nitric acid, hydrogen peroxide, and alkyl hydroperoxides, which may have low energy efficiency and selectivity as well as generate environmentally hazardous waste and by-products [1]. Oxidation using molecular oxygen is very attractive because it is inexpensive, readily available, and environmentally benign.

Transition metal ions, such as Co^{3+}, Mn^{3+}, and Fe^{3+}, substituted aluminophosphates MeAPO-n are promising catalysts for the selective oxidation of cyclohexane with molecular oxygen due to both the highly dispersed redox active centers and the unique shape-selectivity in the metal-incorporated aluminophosphates [2]. By introducing Co^{2+} into the framework of AlPO-5, Co-substituted aluminophosphate CoAPO-5 owns the topological structure of AFI and a uni-directional cylindrical channel of 12-membered rings with uniform cross-sections of 0.73 nm along the axis *c* [3]. Upon calcination, at least part of the framework Co^{2+} ions can be oxidized to Co^{3+} to generate the redox active centers. The framework Co^{3+} isomorphously accommodated in the place of Al^{3+} possesses a tetrahedral coordination [4]. The coordinately unsaturated environment favored the redox catalytic reaction, just like the four-coordinated Ti^{4+} in TS-1 [5]. The isolated Co^{3+} in the CoAPO-5 framework would favor the formation of free radicals in the presence of oxygen and cyclohexane, and then promote the selective oxidation of saturated hydrocarbons by molecular oxygen together with proper pore shape and size of the CoAPO-5 molecular sieves.

Performing reactions under supercritical conditions rather than in gas or liquid phase could be an interesting option for improving the conversion, enhancing the reaction rate, increasing throughput, prolonging catalyst lifetime and making the process more environmentally benign [6–8]. Moreover, the addition of proper supercritical fluid (SCF) media can also be used to replace the environmentally undesirable solvents, improve the conversion, and avoid undesirable side products [9–11]. Several works have been published for the oxidation of cyclohexane in the presence of compressed CO_2 [12–14],

* Corresponding author. Tel.: +86 351 4046092; fax: +86 351 4041153.
E-mail address: iccjgw@sxicc.ac.cn (J. Wang).

0920-5861/$ – see front matter © 2005 Elsevier B.V. All rights reserved.
doi:10.1016/j.cattod.2005.09.033

which indicated that it is advantageous to conduct the reaction in supercritical CO_2, for example, the by-products are much less than those in the absence of CO_2. The reaction products can be made to condense by manipulating the phase behavior circumventing unnecessary side reactions, and the reaction rates and conversions can thus be manipulated by adjusting the operating conditions of temperature and pressure and feed composition near the mixture critical point.

In this work, CoAlPO-5 with different Co contents was hydrothermally synthesized. The tetrahedral Co^{2+} in the lattice framework was evidenced by various spectroscopic characterizations, which could be partially oxidized to Co^{3+} to form redox centers upon calcination. Over CoAPO-5, the selective oxidation of cyclohexane was carried out with CO_2 as an additional solvent under supercritical conditions. Because the operation in the regions near the critical point was most desirable to make most of the unique characteristics of SCF [8], the different phase regions were categorized by the critical properties of the nominal reacting mixture (cyclohexane + nitrogen + carbon dioxide + -cyclohexanol + cyclohexanone + water) that varies with the reaction extent. On the basis of this categorization, a comparative study on the cyclohexane oxidation over CoAPO-5 in different phases was conducted and a relationship of the reaction behaviours with the addition of CO_2 was then proposed.

2. Experimental

2.1. Synthesis

CoAPO-5 molecular sieves with different cobalt contents were synthesized hydrothermally with triethylamine (TEA) as the organic template by the verified method [15]. The gel composition was $xCo_2O_3{\cdot}(1-x)Al_2O_3{\cdot}P_2O_5{\cdot}1.4TEA{\cdot}35H_2O$, where x referred to the molar ratio of Co to P in the initial gel. In a typical synthesis process, $Co(NO_3)_2{\cdot}6H_2O$ was first dissolved in the aqueous solution of H_3PO_4, and pseudoboehmite (as Al source) was then introduced with continuous stirring. TEA was then added dropwise and a homogeneous gel was thus formed. After that, the gel formed in this way was stirred continuously for 1 h and transferred to a 100 ml stainless steel Teflon-lined autoclave, where the crystallization was conducted under static condition at 200 °C for 24 h. The solid products were then washed and dried at 120 °C overnight, and finally, the template-free powder product in green color was obtained by calcination at 550 °C in air for 6 h.

2.2. Characterization

X-ray powder diffraction (XRD) was preformed on a Rigaku D/max-2500 X-ray diffraction spectrometer. The diffraction patterns were obtained in the 2θ range of 5–40° by using Cu Kα radiation (0.15418 nm, 40 kV, and 100 mA).

Ultraviolet and visible diffuse reflectance spectroscopy (UV–vis DRS) was collected on a Shimadzu UV-2101PC spectrophotometer equipped with an integration sphere. The spectra were recorded using $BaSO_4$ powder as a reference in the region of 200–800 nm.

X-ray absorption near edge structures (XANES) spectroscopy was performed on the 4WIB beam line using synchrotron radiation from the storage ring running at 2.2 GeV with an average current of 50 mA in XAFS station (BEPC). The data were collected in transmission mode through a double crystal monochromatic (Si(1 1 1)) using ion chamber detector.

2.3. Determination of the critical properties of the reacting mixture

As described previously [16], following reaction scheme is assumed to prepare the nominal reacting mixture for measuring the critical properties:

$$2C_6H_{12} + \tfrac{3}{2}O_2 \rightarrow C_6H_{12}O + C_6H_{10}O + H_2O$$

considering that only small amounts of by-products are observed for the selective oxidation of cyclohexane in the presence of CO_2 [11] and both cyclohexanone and cyclohexanol owns the analogous selectivity and critical properties. The composition of the nominal reacting mixture (cyclohexane + nitrogen + carbon dioxide + cyclohexanol + cyclohexanone + water, where nitrogen is regarded as the homomorphous stand-in of oxygen) was then determined according to the initial reactants constitutes (cyclohexane, nitrogen/oxygen and CO_2) and the reaction extent (conversion of cyclohexane). The critical properties of the mixtures were then measured with the same view cell and procedures as described previously [10,16].

2.4. Catalytic tests and analytical procedures

The oxidation of cyclohexane over CoAPO-5 in the compressed CO_2 was carried out in a stainless steel batch reactor of 14.13 cm^3. Before each test, the catalyst and cyclohexane as well as small amounts of the initiator tetrabutyl hydroperoxide (TBHP) were added, and then oxygen and CO_2 were purged to the reactor. The mole fractions of cyclohexane, oxygen and CO_2 in a typical mixture of initial reactants are 0.15, 0.15, and 0.70, respectively. The usages of catalyst and the initiator TBHP is 2.0 wt% and 0.2 wt% of cyclohexane, respectively. The volume occupied by catalyst and the volume of the pipe connected to the pressure sensor was corrected for the calculation of the apparent density. Once the reactants and catalyst were charged, the reactor was set in an air bath at certain temperature with a fluctuation about ±0.2 °C and the mixture in the reactor was stirred intensively with a magnetic stirrer. After the reaction lasted for certain time, the reactor was placed in a freezer at about 0 °C for 1 h, and then CO_2 and O_2 was allowed to be released slowly. Mass balance test indicated that the amounts of reactants and products entrained by the gases were negligible.

For comparison, the reaction in the absence of CO_2 was carried out in a 100 cm^3 autoclave equipped with heating jacket, stirrer, liquid separator, and sampling valve. Fifty grams cyclohexane, 0.5 g CoAPO-5, and 0.1 g TBHP as initiator were introduced into the reactor. The reactor was charged with 1.5 MPa O_2, heated to 130 °C within 30 min with stirring, and kept at this temperature for given time.

The products were analyzed on an FID gas chromatograph (Shimadzu GC-8A) equipped with a 3 m × 3.2 mm packed column of Carbowax 20 M on Chromosorb WAW 80/100 and argon as carrier gas, and cyclooctane was used as the internal standard. Cyclohexane, cyclohexanone, and cyclohexanol were quantified directly; cyclohexyl hydroperoxide (CHHP) was estimated through both direct sampling and injection after reducing to cyclohexanol with triphenylphosphine (PPh_3) because it decomposed partially upon injection [17]; the acids formed were determined by detecting the methyl esters after its esterification with $BF_3 + CH_3OH$ [18].

3. Results and discussion

3.1. Properties of CoAPO-5

The XRD patterns of as-synthesized CoAPO-5 molecular sieves with four Co contents (Co/P = 0.01, 0.05, 0.08, 0.10) were shown in Fig. 1. The XRD patterns illustrated the rather high crystallinity and purity of the molecular sieves, as no extra peaks related to impurities such as transition metal oxide were observed, although the degree of crystallization may vary with the Co content. The crystallinity of CoAPO-5 improves remarkably with the increase of Co/P ratio from 0.01 to 0.05, while the degree of crystallization decreases with further increase of Co content. The optimal Co/P ratio for the synthesis of CoAPO-5 is about 0.05, and higher Co content may result in a great deal of extra framework species [19] that may deposit on the pore interior surface and influence the framework accordingly.

The UV–vis DRS spectra (Fig. 2) of the as-synthesized CoAPO-5 showed the presence of an intense triplet band between 520 and 650 nm due to the $^4A_2 \rightarrow {}^4T_1(P)$ transition of high spin of tetrahedral Co^{2+} (d^7) [20,21], which indicated the existence of tetrahedral cobalt in the framework of CoAPO-5 molecular sieves. It is noticeable that the intensity of the triplet band increased monotonously with the Co concentration in the initial gel, which suggested that with the Co/P value below 0.10, the more cobalt introduced into the initial gel, the more Co^{2+} incorporated in the framework.

After calcination, the triplet band attributed to tetrahedral Co^{2+} decreased accompanied by the appearance of two new

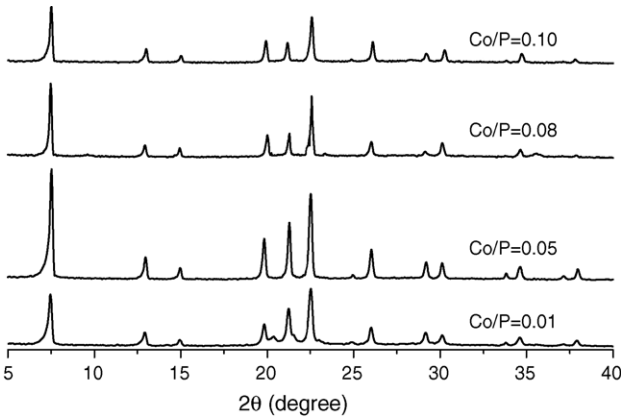

Fig. 1. XRD patterns of CoAPO-5 with different Co contents.

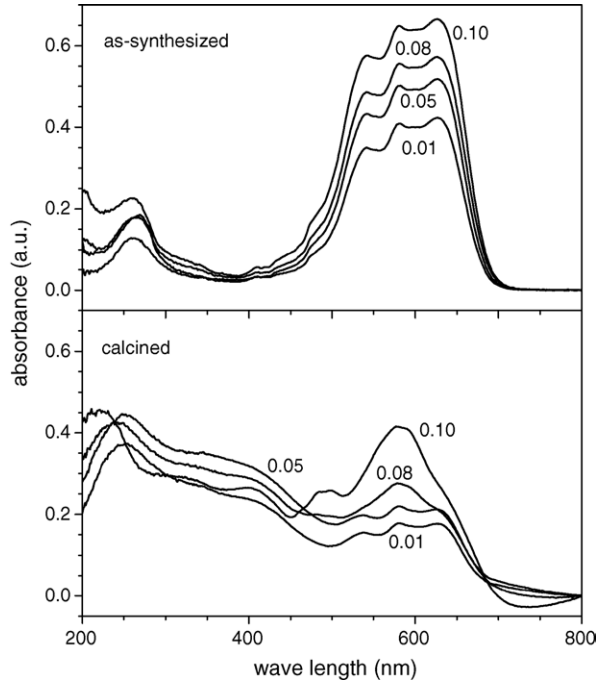

Fig. 2. UV–vis DRS spectra of as-synthesized and calcined CoAPO-5 prepared with the different Co/P ratios of 0.10, 0.08, 0.05, and 0.01 in the initial gel.

absorbance bands around 320 nm and 390 nm, which originated from the characteristic absorption of tetrahedral Co^{3+} in the framework of CoAPO-5 [20–23]. This suggested an oxidation of Co^{2+} to Co^{3+} upon calcination. A maximum amount of Co^{3+} was observed on CoAPO-5 with a Co/P ratio of 0.05. However, the presence of significant amounts of high-spin octahedral Co^{2+} in the calcined CoAPO-5 (Co/P = 0.10) evidenced by the shoulder at 480 nm indicated that part of tetrahedral Co^{2+} has changed to the octahedral coordination upon calcination [24]. This may result from the distortion of the framework or the exclusion of Co^{2+} from the lattice to the extra framework sites.

A pre-edge structure can be identified from the normalised Co *K*-edge XANES spectra of as-synthesized CoAPO-5 (Fig. 3). The shape of *K*-edge and the pre-edge resonance are characteristic for the local symmetry of the investigated atom and can be used as

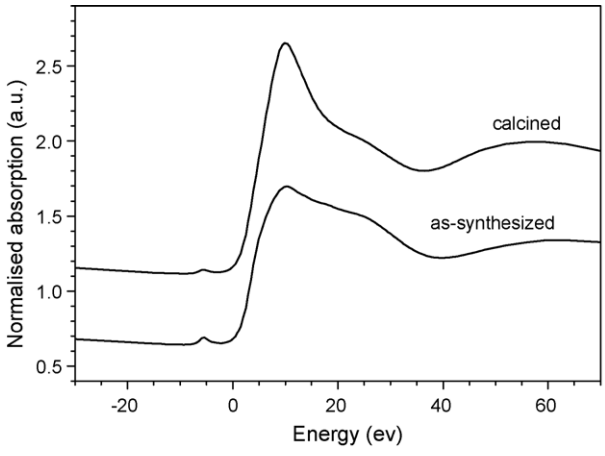

Fig. 3. Normalized Co *K*-edge profiles of CoAPO-5 (Co/P = 0.10) samples. The energy scale is relative to the Co *K*-edge in the metal (7709.0 eV).

Table 1
Energy shift ΔE_K of the Co *K*-edge and an evaluation of the average Co oxidation number and the fraction of Co cations in the frameworks of CoAPO-5[a]

CoAPO-5 (Co/P = 0.10)	ΔE_K (eV)	Co oxidation number	Fraction of Co cations (%)	
			Co^{2+}	Co^{3+}
As-synthesized	4.4(8)	+2.0(0)	100	0
Calcined	4.9(6)	+2.2(2)	78	22

[a] Metal Co with a oxidation number of 0 was used as the standard and has a ΔE_K of 0.0; numbers in parentheses correspond to the standard error in the last significant digit.

fingerprints for the identification of its local structure. The existence of pre-edge peak originated from 1s → 3d transition of Co can be traced back to the structure of cobalt species. The transition is forbidden in the octahedral coordinated Co species (e.g. CoO), while it is permitted in the tetrahedral structure. This suggested a four-fold coordination structure of Co and thence the incorporation Co in the framework [23,25]. After the removal of organic templates by calcination, the intensity of the pre-edge structure decreases slightly, indicating a distortion of the coordination environment of Co upon calcination. This suggested again that part of Co in lattice framework is unstable and may be expulsed to the extra-framework under thermal treatments as revealed by the UV–vis DRS spectra.

After calcination, a slight shift of the absorption edge to the higher energy can be distinguished from the XANES spectra (Fig. 3). A linear relation between the edge shift and the valence state has been established for the atoms with the same type of ligands [26], and shifts of 1.5–3 eV per valence have been reported for cobalt atoms [23]. Using the absorption edge of metal Co (7709 eV) as the reference, the *K*-edge energy shifts (ΔE_K) to Co^0 for as-synthesized and calcined CoAPO-5 products were given in Table 1. A shift of 0.48 eV to the higher energy after calcination indicated an increase of 0.2 ± 0.02 in the average cobalt oxidation number, which suggested that about 22% of the framework Co^{2+} was oxidized to Co^{3+} upon calcination.

3.2. Categorization of different reaction zones

To make most of the unique characteristics of the reacting medium under supercritical conditions, one must be cognizant of the critical properties of the reacting mixture along with the reaction course [8]. After the critical properties of the nominal

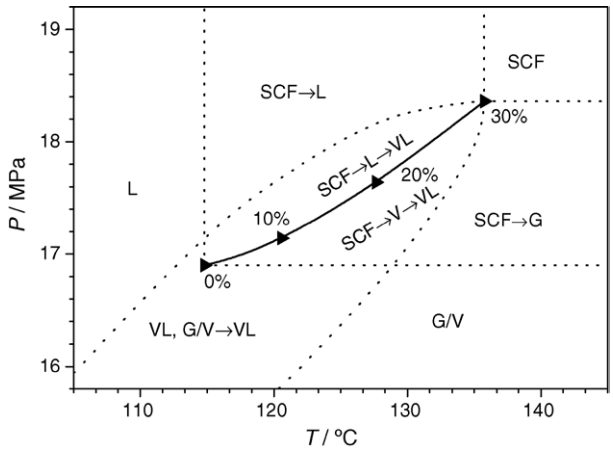

Fig. 4. Phase variance of the reacting mixture during reaction with the initial mole fractions of cyclohexane, oxygen, and CO_2 being 0.15, 0.15, and 0.70, respectively. The solid line with the triangle points represents the critical properties of the reacting mixture with the reaction extent (as the percentage of cyclohexane conversion); the dotted lines reflect the different zones of phase variance.

reacting mixture (cyclohexane + nitrogen + carbon dioxide + -cyclohexanol + cyclohexanone + water) were determined with the composition representing the reaction extent (conversion of cyclohexane) [16], the different phase regions can be categorized as shown in Fig. 4. It is assumed here that the initial mole ratio of cyclohexane to oxygen is 1:1 with an initial mole fraction of CO_2 being 0.70, and the ultimate reaction extent is 30%.

As shown in Fig. 4, the critical properties of the reacting mixture change with the reaction proceeding extent. With the reaction proceeding to a higher cyclohexane conversion, both the critical temperature and the critical pressure shift to a higher value. When the reaction is carried out at a fixed temperature and pressure, the reacting mixture may either lie in a single phase of liquid (L), gas (G), vapor (V) or supercritical fluid (SCF), or present as a region of V–L coexistence (VL). Under certain conditions, the reacting mixture may also endure a phase variance of SCF → L, SCF → G, G/V → VL, SCF → V → VL, or SCF → L → VL.

To ensure that the reaction was carried out in SCF, the reaction temperature and pressure should be higher than the critical point of the ultimate resultant mixture. In the current work, the cyclohexane conversion in most tests was lower than 10%, therefore, the reaction temperature of 121.2 °C is used with the initial mole fraction of cyclohexane, oxygen and CO_2 being 0.15, 0.15, and 0.70, respectively. As shown in Table 2, the reactions

Table 2
Conversion and selectivity of cyclohexane oxidation with the apparent density over CoAPO-5 (Co/P = 0.05) in the presence of CO_2[a]

Apparent density (g/cm^3)	Pressure (MPa)	Phase variances	Conversion (%)	-ol selectivity (%)	-one selectivity (%)
0.27	10.93	G/V	8.7	54.0	44.0
0.33	13.35	G/V	7.4	50.2	48.3
0.43	15.70	G/V	6.2	47.5	51.2
0.48	17.18	SCF → G	5.3	44.0	55.0
0.55	19.87	SCF	4.2	40.2	58.9
0.61	22.22	SCF	3.7	37.4	62.1

[a] The initial mole fractions of cyclohexane, oxygen, and CO_2 in the reacting mixture were 0.15, 0.15, and 0.70; catalyst and initiator TBHP (2.0% and 0.2 wt% of cyclohexane, respectively) was introduced; the reaction lasted for 15 h at 121.2 °C.

Table 3
Cyclohexane oxidation on CoAPO-5 with different Co contents in the absence of CO_2[a]

Co/P ratio	Time (h)	Conversion (%)	Product distribution (%)					
			CHHP	-ol	-one	Others[b]	-ol + -one	-one/-ol
0.08	8	6.8	11.5	35.4	43.6	9.5	79.0	1.23
	24	13.9	–	31.5	53.6	14.9	85.1	1.70
0.05	8	8.0	13.3	36.6	44.7	7.2	81.3	1.22
	24	14.7	–	30.1	58.4	11.5	88.5	1.94
0.01	8	5.9	10.1	38.0	45.4	6.5	83.4	1.20
	24	11.3	–	34.3	55.4	10.3	89.7	1.62

[a] Fifty grams cyclohexane, 0.5 g catalyst, 0.1 g TBHP as initiator, and 1.5 MPa O_2 were charged into 100 cm^3 autoclave for each test; reactions lasted for 8 h or 24 h at 130 °C.
[b] Others included mainly adipic acid and valeric acid.

can be conducted in the regions of SCF, SCF → G, and G/V by controlling the density of the reacting mixture (to adjust the reaction pressure) at this temperature and initial composition.

3.3. Reactions in the absence and presence of carbon dioxide

For comparison, cyclohexane oxidation in the absence of CO_2 was viewed on CoAPO-5 molecular sieves with different Co contents (Table 3). Co content in the framework had a significant influence on the reactivity. The total selectivity of cyclohexanol and cyclohexanone decreased slightly with the increase of Co/P ratio from 0.01 to 0.08, while the CoAPO-5 with a Co/P ratio of 0.05 gave the highest conversion of cyclohexane. The catalytic activity of CoAPO-5 may be related to its crystallinity. CoAPO-5 with a Co/P ratio of 0.05 that owns the highest crystallinity also exhibits the highest conversion of cyclohexane.

The major products of the oxidation reaction in the absence of CO_2 were cyclohexanol and cyclohexanone; CHHP, the intermediate of the cyclohexane oxidation, appeared only for reactions in short duration and converted further to cyclohexanol and cyclohexanone if the reaction lasted longer. The by-products, mainly adipic and valeric acids, increased significantly with the reaction time. The initiator TBHP is used to accelerate the generation of intermediates with free radicals and reduce the induction time without changing the distribution of the reaction products [27]. Without the initiator, cyclohexane conversion is only about 2.1% after reaction for 24 h with CoAPO-5 (Co/P ratio is 0.05) as catalyst; it is elevated to 14.7% with a similar products distribution by adding small amounts of TBHP as the initiator.

The conversion and selectivity for the reaction over CoAPO-5 (Co/P = 0.05) in the absence and presence of CO_2 (apparent density $\rho = 0.27$ g/cm^3) were compared in Fig. 5. With the addition of compressed CO_2, the selectivity to cyclohexanol and cyclohexanone was enhanced, while the by-products, such as adipic acid and valeric acid, were suppressed considerably.

3.4. Effects of the apparent density on reaction in the presence of carbon dioxide

As shown in Table 2 and Fig. 6, the conversion of cyclohexane and selectivity of cyclohexanol and cyclohexanone changed significantly with the phase variance and the apparent density. Unlike in the case of Tian et al.'s work on the benzene alkylation [8], the phase variance from G/V to SCF → G and SCF is not so acute (without enduring the V–L transformation), therefore, the conversion and selectivity here do not show any sharp distortion with the apparent density. The conversion decreased with the increase of the apparent density. This may be ascribed to that more active sites would be

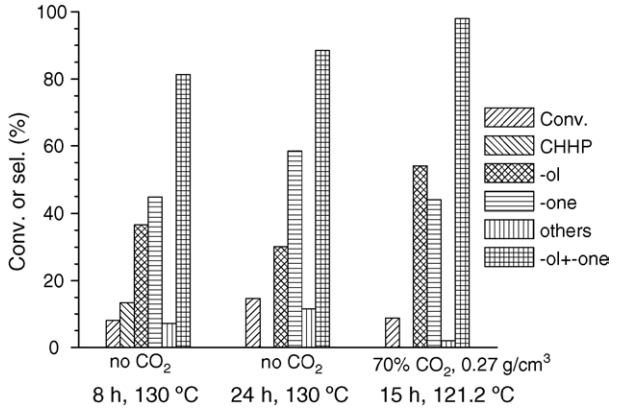

Fig. 5. Comparison of conversion and selectivity in the absence and presence of CO_2 over CoAPO-5 (Co/P = 0.05).

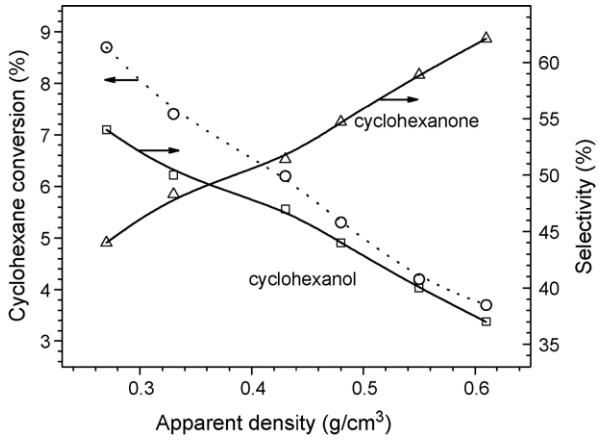

Fig. 6. Conversion and selectivity of cyclohexane oxidation with different apparent densities over CoAPO-5 (Co/P = 0.05): the initial mole fractions of cyclohexane, oxygen, and CO_2 were 0.15, 0.15, and 0.70, respectively; all the reactions lasted for 15 h at 121.2 °C.

occupied by CO_2 and less active sites leaved available for the reactants under higher density of CO_2, which is not favorable for the cyclohexane conversion.

However, the amounts of by-products decreased with the increase of the apparent density. At lower pressure ($\rho < 0.33$ g/cm^3), the selectivity of cyclohexanol is higher than that of cyclohexanone and it decreased with the increase of pressure, while the selectivity of cyclohexanone was enhanced at higher density. This may be due to the intrinsic properties of reactants, products, and the solvent. The polarity of cyclohexanol molecule is stronger than that of cyclohexanone molecule; the higher density of non-polar CO_2, especially under supercritical condition, is then favorable for the transformation of cyclohexanol to cyclohexanone. Thus, it is suggested that a selective oxidation of cyclohexane to the objective products is available by choosing proper solvent and reaction conditions.

4. Conclusions

A series of CoAPO-5 with different Co contents were hydrothermally synthesized. The tetrahedral Co^{2+} in the lattice framework was evidenced by various spectroscopic characterizations, and a consistence of the content of Co^{2+} in frameworks with that in the initial gel was suggested. Co^{2+} in the framework could be partially oxidized to Co^{3+} to form redox centers upon calcinations.

The different phase regions were categorized by the critical properties of the nominal reacting mixture, and the selective oxidation of cyclohexane over CoAPO-5 was carried out with CO_2 as an additional solvent under supercritical conditions. It was proved that CoAPO-5 is an effective catalyst for the selective oxidation of cyclohexane to cyclohexanol and cyclohexanone; in the compressed CO_2, the total selectivity of objective products increased and the by-products were compressed considerably. The conversion of cyclohexane decreased, while the selectivity to cyclohexanol and cyclohexanone increased with the increase of the apparent density. A selective oxidation of cyclohexane to the objective products is available by the elaborate choice of the proper solvent and reaction conditions.

Acknowledgments

The authors are grateful for the financial support of the Sate Key Fundamental Research Project, the Natural Science Foundation of China (20473110) and Natural Science Foundation of Shanxi Province, and the assistance in XANES characterization from BEPC Synchrotron Radiation Laboratory.

References

[1] T. Maschmeyer, J.M. Thomas, G. Sankar, R.D. Olyroyd, I.J. Shannon, J.A. Kleptko, A.F. Masters, J.K. Beattie, C.R.A. Catlow, Angew. Chem. Int. Ed. 36 (1997) 1639.
[2] R. Raja, G. Sankar, J.M. Thomas, J. Am. Chem. Soc. 121 (1999) 11926.
[3] I.W.C.E. Arends, R.A. Sheldon, M. Wallau, U. Schuchardt, Angew. Chem. Int. Ed. 36 (1997) 1144.
[4] J.M. Thomas, R. Raja, G. Sankar, R.G. Bell, Nature 398 (1999) 227.
[5] G. Sankar, J.M. Thomas, C.R.A. Catlow, Top. Catal. 10 (2000) 255.
[6] P.E. Savage, S. Gopalan, T.I. Mizan, C.J. Martino, E.E. Brock, AIChE J. 41 (1995) 1723.
[7] A. Baiker, Chem. Rev. 99 (1999) 453.
[8] Z. Tian, Z. Qin, M. Dong, G. Wang, J. Wang, Catal. Commun. 6 (2005) 385.
[9] Z. Qin, J. Liu, J. Wang, Fuel Process. Technol. 85 (2004) 1175.
[10] T. Hu, Z. Qin, G. Wang, X. Hou, J. Wang, J. Chem. Eng. Data. 49 (2004) 1809.
[11] Z. Hou, B. Han, X. Zhang, H. Zhang, Z. Liu, J. Phys. Chem. B 105 (2001) 4510.
[12] P. Srinivas, M. Mukhopadhyay, Ind. Eng. Chem. Res. 36 (1997) 2066.
[13] E. Sahle-Demessie, M.A. Gonzalez, J. Enriquez, Q. Zhao, Ind. Eng. Chem. Res. 39 (2000) 4858.
[14] Z. Hou, B. Han, L. Gao, Z. Liu, G. Yang, Green Chem. 4 (2002) 426.
[15] H. Robson, Verified Syntheses of Zeolitic Materials, Elsevier, Netherlands, 2001, p. 96.
[16] R. Zhang, Z. Qin, G. Wang, M. Dong, X. Hou, J. Wang, J. Chem. Eng. Data 50 (2005) 1414.
[17] G.B. Shulpin, D. Attanasio, L. Suber, J. Catal. 142 (1993) 147.
[18] R. Raja, P. Ratnasamy, Catal. Lett. 48 (1997) 1.
[19] W. Fan, R.A. Schoonheydt, B.M. Weckhuysen, Chem. Commun. 22 (2000) 2249.
[20] Q. Gao, B.M. Weckhuysen, R.A. Schoonheydt, Microporous Mesoporous Mater. 27 (1999) 75.
[21] R.A. Schoonheydt, R. De Vos, J. Pelgrims, H. leeman, in: P.A. Jacobs, R.A. van Santen (Eds.), Zeolites, Facts, Figures, Elsevier, Amsterdam, 1989, p. 559.
[22] L. Canesson, I. Arcon, S. Caldarelli, A. Tuel, Microporous Mesoporous Mater. 26 (1998) 117.
[23] P.A. Barrett, G. Sankar, C.R.A. Catlow, J.M. Thomas, J. Phys. Chem. 100 (1996) 8977.
[24] W. Fan, R.A. Schoonheydt, B.M. Weckhuysen, Phys. Chem. Chem. Phys. 3 (2001) 3240.
[25] J. Chen, G. Sankar, J.M. Thomas, R. Xu, G. Neville-Greaves, D. Waller, Chem. Mater. 4 (1992) 1373.
[26] J. Wong, F.W. Lytle, R.P. Messmer, D.H. Maylotte, Phys. Rev. B 30 (1984) 5596.
[27] R. Raja, G. Sankar, J.M. Thomas, J. Am. Chem. Soc. 121 (1999) 11926.